Localized surface plasmon resonance immunoassay and verification using surface-enhanced Raman spectroscopy

Chanda Ranjit Yonzon, Xiaoyu Zhang, and Richard P. Van Duyne
Northwestern University, Dept. of Chemistry, 2145 Sheridan Rd, Evanston, IL, USA 60208

ABSTRACT

This work exploits the localized surface plasmon resonance (LSPR) spectroscopy of noble metal nanoparticles to achieve sensitive and selective detection of biological analytes. Noble metal nanoparticles exhibit an LSPR that is strongly dependent on their size, shape, material, and the local dielectric environment. The LSPR is also responsible for the intense signals observed in surface-enhanced Raman scattering (SERS). Ag nanoparticles fabricated using the nanosphere lithography (NSL) technique exploits this LSPR sensitivity as a signal transduction method in biosensing applications. The current work implements LSPR biosensing for the anti dinitrophenyl (antiDNP) immunoassay system. Upon forming the 2,4 dinitrobenzoic acid /antiDNP complex, this system shows a large LSPR shift of 44 nm when exposed to antiDNP concentration of 1.5×10^{-6} M. In addition, due to the unique molecular characteristics of the functional groups on the biosensor, it can also be characterized using SERS. First, the nanoparticles are functionalized with a mixed self-assembled monolayer (SAM) comprised of 2:1 octanethiol and 11-amino undecanethiol. The SAM is exposed to 2,4-dinitrobenzoic acid with the 1-ethyl-3-[3-dimethylaminopropyl]carbodiimide hydrochloride (EDC) coupling reagent. Finally, the 2,4-dinitrophenyl terminated SAM is exposed to various concentration of antiDNP. LSPR shifts indicate the occurrence of a binding event. SER spectra confirm binding of 2,4 dinitrobenzoic acid with amine-terminated SAM. This LSPR/SERS biosensing method can be generalized to a myriad of biologically relevant systems.

Keywords: Localized surface plasmon resonance, surface-enhanced Raman spectroscopy, nanosphere lithography, self-assembled monolayer, anti dinitrophenyl, biosensor

1. INTRODUCTION

Biosensors based on propagating surface plasmon resonances (SPR) at flat, thin Au films have been widely used to detect a variety of biological molecules on functionalized surfaces. SPR sensors have been used to study hundreds of biomolecular interactions, including cell adhesion,[1] receptor ligand,[2,3] antibody-antigen,[4] protein-carbohydrate,[5] protein-DNA,[6] and DNA-DNA[7] interactions. Despite the advantages that SPR sensors provide, they face some fundamental challenges: 10μm x 10μm pixel size, complex construction, large sample volume, long-range distance dependence (~200 nm), and kinetic measurements limited by planar diffusion. The Van Duyne group has developed localized surface plasmon resonance (LSPR) sensors using noble metal nanoparticles that retain the optical properties of SPR sensors. Additionally, the LSPR sensors have small pixel size (one nanoparticle), simple construction, small sample volume, short range distance dependence (~6 nm), and kinetic measurements that are dependent upon radial diffusion.[8,9]

LSPR nanosensors capitalize on the fact that noble metal nanoparticles exhibit a strong UV-vis extinction (absorption and Rayleigh scattering) band that is not present in the bulk material.[10-17] This extinction band is a direct consequence of the excitation of the LSPR, which is the collective oscillation of the conduction electrons in the metal nanoparticle. The peak extinction wavelength of this band, λ_{max}, is dependent upon the size, shape, material, and dielectric environment of the nanoparticles.[10-17] The simplest theoretical model for the extinction, $E(\lambda)$, of a spherical nanoparticles is given by Equation 1,[18]

Proceedings of SPIE Vol. 5224 Nanomaterials and Their Optical Applications, edited by Guozhong Cao, Younan Xia, Paul V. Braun (SPIE, Bellingham, WA, 2003) · 0277-786X/03/$15.00

$$E(\lambda) = \frac{24\pi^2 N a^3 \varepsilon_m^{3/2}}{\lambda \ln(10)} \left[\frac{\varepsilon_i}{(\varepsilon_r + 2\varepsilon_m)^2 + \varepsilon_i^2} \right] \quad (1)$$

where N is Avagadro's number, a is the radius of the sphere, ε_m is the external dielectric constant, and ε_i and ε_r and real and imaginary portion of dielectric constant of the metal. The working principle of LSPR sensors is that changes in the local dielectric environment caused by molecular binding events or adsorption cause a shift in the LSPR λ_{max}.

Although LSPR sensors can be used to monitor the binding of macromolecules to functionalized nanoparticle surfaces, extinction spectroscopy does not allow for specific identification of the chemical entity. Vibrational spectroscopy, on the other hand, is capable of revealing molecular characteristics of the analyte. SERS, discovered by Van Duyne et al. in 1977,[19] shows a 10^6-10^{14} enhancement in effective Raman cross-section when the analyte is bound or close to the surface of a noble metal nanoparticles.[20-22] This enhancement is a result of the strong local electromagnetic fields near the surface of the nanoparticle that are generated by exciting the LSPR.[23] SERS, similar to Raman scattering, is an inelastic scattering process in which photons incident on a sample transfer energy to or from the sample's vibrational or rotational modes. Individual bands in a SERS spectrum are characteristic of a specific molecular motion. As a result, each chemical entity has its own unique Raman signature. SERS is an important technique that can display intrinsic interfacial sensitivity and selectivity. SERS has been used to study quantitative and qualitative study in biological systems.[24] By combining SERS and LSPR spectroscopy, the binding of molecules can be confirmed on the nanosensors.

Previously, the efficacy of LSPR sensors has been demonstrated for two ligand/receptor systems: (1) biotin/streptavidin,[9] and (2) biotin/antibiotin.[25] The latter is the first example of a real-time immunoassay using the LSPR signal transduction mechanism. These studies have demonstrated that detection on LSPR sensors is highly selective and sensitive (the detection limit of biotin/streptavidin complex is 1pM)[9] as dictated by the value of the affinity binding constant. In this paper, we have used LSPR spectroscopy to study the binding event of a biomolecule and its complimentary ligand/receptor as well as the use of SERS to study the fabrication of a nanobiosensor.

2. EXPERIMENTAL

2.1 Materials. Ag (99.99%, 0.04 in. diameter) was purchased from D.F. Goldsmith (Evanston, IL). Glass substrates were 18-mm-diameter, no. 2 coverslips from Fisher Scientific (Fairlawn, VA). Pretreatment of glass substrates required H_2SO_4, H_2O_2, and NH_4OH, all purchased from Fisher Scientific (Fairlawn, VA). Surfactant-free, white carboxyl-substituted polystyrene latex nanospheres with diameters of 390 nm ± 19.5 nm were received as a suspension in water from Duke Scientific (Palo Alto, CA). Tungsten vapor deposition boats were purchased from R. D. Mathis (Long Beach, CA). 1-octanethiol and 2,4-dinitrobenzoic acid were purchased from Aldrich (Milwaukee, WI). Monoclonal antiDNP, 1-ethyl-3-[3-dimethylaminopropyl]carbodiimide hydrochloride (EDC), phosphate buffered saline (PBS), pH=7.4 were obtained from Sigma (St. Louis, MO). 11-amino 1-undecanethiol hydrochloride was purchased from Dojindo Molecular Technologies (Japan). Absolute ethanol was purchased from Pharmco (Brookfield, CT).

2.2 Nanosphere Lithography. Glass substrates were pretreated in two steps (1) piranha etch, 1:3 30%H_2O_2:H_2SO_4 at 80ºC for half an hour to clean the substrate, and (2) base treatment, 5:1:1 H_2O:NH_4OH:30%H_2O_2 with sonication for 1 hr, was used to render the surface hydrophilic. Approximately 2 µl of undiluted nanosphere solution (10% solid) was drop-coated on the pretreated glass substrate and allowed to dry in ambient conditions to form 2D hexagonally packed array. Ag was deposited in a modified Consolidated Vacuum Corporation vapor deposition system with a base pressure of 10^{-7} Torr. The mass thickness of 50 nm and deposition rate for each film was measured using a Leybold Inficon XTM/2 quartz-crystal microbalance (QCM) (East Syracuse, NY). After Ag deposition, polystyrene nanospheres were removed by sonication in absolute ethanol for 3 min.

2.3 Ag film over nanosphere (FON). Hexagonal arrays of polystyrene spheres with 390 nm diameters were made on a glass substrate as mentioned above. Fabrication of AgFONs was accomplished by depositing 200 nm of Ag over the 2D arrays of nanospheres.

2.4 Atomic Force Microscopy (AFM). AFM was used to obtain topographic images of the nanoparticle arrays. The images were taken under ambient conditions with Digital Instruments Nanoscope IV microscope with a Nanoscope IIIa controller operating in tapping mode. Etched Si nanoprobe tips (TESP, Digital Instruments, Santa Barbara, CA) were used. These tips had resonance frequencies between 280 and 320 kHz and were conical in shape, with cone angle of 20º and an effective radius of curvature at the tip of 10 nm.

2.5 Ultraviolet-visible Extinction Spectroscopy. UV-vis extinction measurements were taken using an Ocean Optics (Dunedin, FL) SD2000 fiber optically-coupled spectrometer. All spectra in this study were from macroscopic measurements obtained in transmission mode using unpolarized white light with probe diameter of 4 mm. A home built flow cell[8] was used to control the surrounding environment of Ag nanoparticles.

2.6 Surface-enhanced Raman spectroscopy (SERS). A Spectra Physics Model 120 HeNe laser was used for 632.8 nm excitation. In the laser path, a 632.8 Edmund Scientific (Barrignton, NJ) interference filter and a Kaiser (Ann Arbor, MI) holographic notch filter were placed. The scattered light was coupled to an Acton Research Corporation (Acton, MA) VM-505 monochromator equipped with a Roper Scientific (Trenton, NJ) Spec-10:400B liquid-N_2-cooled CCD detector. The spectrometer was calibrated using the emission lines of a Ne lamp.

2.7 Analysis of SERS data. Data processing was done using MATLAB (Math Works, Inc., Natick, MA) and Microsoft Excel (Microsoft Corp., Redmond, WA). Prior to data analysis, cosmic rays were removed from the spectra using a derivative filter. The slowly varying background, commonly seen in SERS experiments, was removed by subtracting a fourth-order polynomial.

3. RESULTS AND DISCUSSION

3.1 Fabrication of the LSPR Nanosensor. Ag nanotriangles were created using nanosphere lithography (NSL) on a glass substrate, and the nanotriangles were functionalized as shown in Figure 1. Nanotriangles were functionalized by

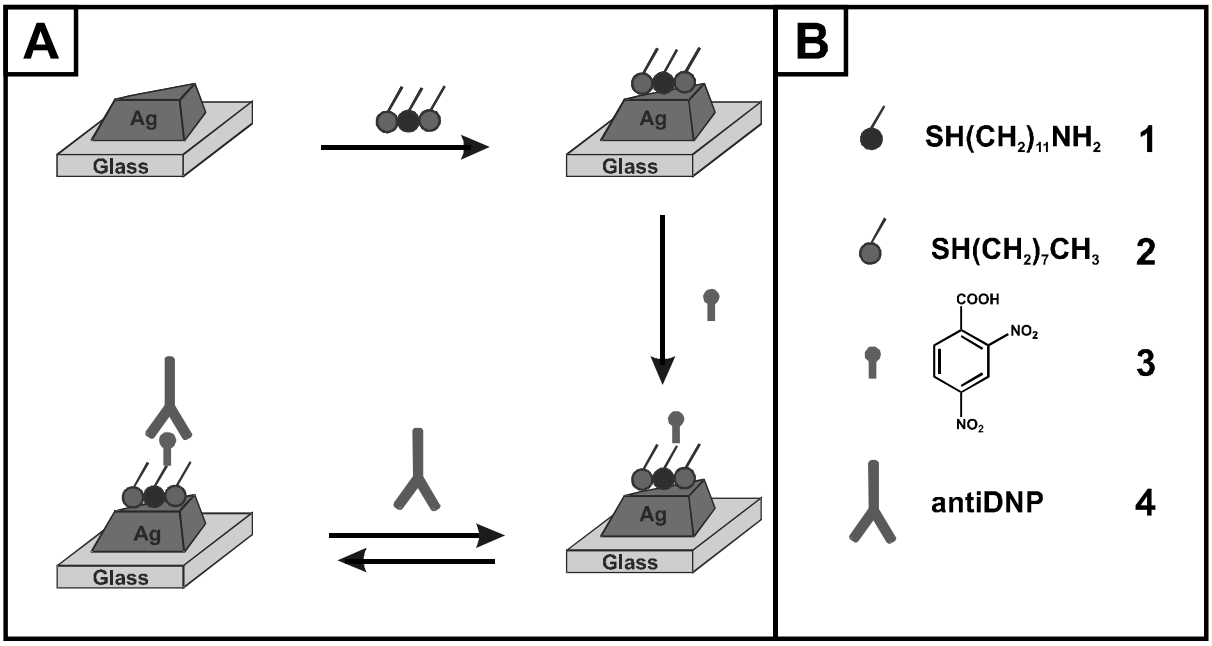

Figure 1: A) Schematic of Ag nanoparticle functionalization subsequently. NSL-fabricated Ag nanoparticles are exposed to a mixture of 2:1 octanethiol (B-1): 11-aminoundecanethiol (B-2). 2,4 -dinitrobenzoic acid (B-3) was covalently linked to the amine-terminated SAM. The 2,4 -dinitrobenzoic acid-functionalized sample was exposed to antiDNP (B-4).

exposing the sample to 1 mM 2:1 octanethiol:11-aminoundecanethiol for 48 hours to ensure a well-ordered SAM. After rinsing in ethanol, the sample was dried under N_2. Octanethiol (Figure 1B-2) was used as a packing material while 11-aminoundecanethiol (Figure 1B-1) was used to covalently attach DNBA (Figure 1B-3) using EDC as a coupling reagent. The covalent attachment of DNBA was accomplished by exposing the SAM-functionalized nanotriangles to 1mM DNBA and 1mM EDC for 3 hours to form an amide bond. The immunoassay was performed by incubating the DNBA-modified sample in antiDNP (Figure 1B-4) solutions for 20 minutes.

All the spectroscopic measurements were performed under nitrogen in ambient conditions. The LSPR response to various antiDNP concentrations is depicted in Figure 2. The LSPR λ_{max} of a DNBA-functionalized was measured to be 653 nm (Figure 2A). After exposure to 1.5 x 10^{-6} M antiDNP, the LSPR λ_{max} was 697 nm, which is a red shift of 44 nm. When the DNBA-functionalized surface is exposed to an antiDNP concentration of 1.5 x 10^{-9} M, the observed shift is 2 nm (Figure 2B). AFM images were taken of the samples after they had been functionalized with DNBA and antiDNP. The AFM tapping mode image of NSL-fabricated nanotriangles on glass after being modified with DNBA showed the average height of 51.4 nm (Figure 3A). Figure 3B shows height increase of 2 nm when the DNBA- functionalized nanotriangles were exposed to 1.5 x 10^{-9} M antiDNP.

These results demonstrate that the NSL-fabricated nanobiosensor is a sensitive detector of immunoglobulins. The binding of antiDNP to surface-tethered DNBA is indicated by a large red shift in the LSPR of the Ag nanoparticles. LSPR shift is dependent upon the refractive index change of the environment, and consequently it is dependent upon the surface concentration of the bound macromolecules. AntiDNP concentration of 1.5 x 10^{-6} M showed a 44 nm shift. This wavelength shift results from saturation antiDNP coverage, confirmed by AFM imaging (not shown) with an additional height increase of 5.9 nm. An antiDNP concentration of 1.5 x 10^{-9} M showed only 2 nm shift in LSPR, which was the lowest detectable LSPR shift for this system. The additional height increase for this antiDNP concentration was only 2 nm.

3.2 LSPR wavelength shift as a function of AntiDNP concentration. The binding curve was generated by exposing the nanotriangles to antiDNP concentrations ranging from 1.5 x 10^{-6} M to 2.5 x 10^{-10} M (Figure 4). Each solid point

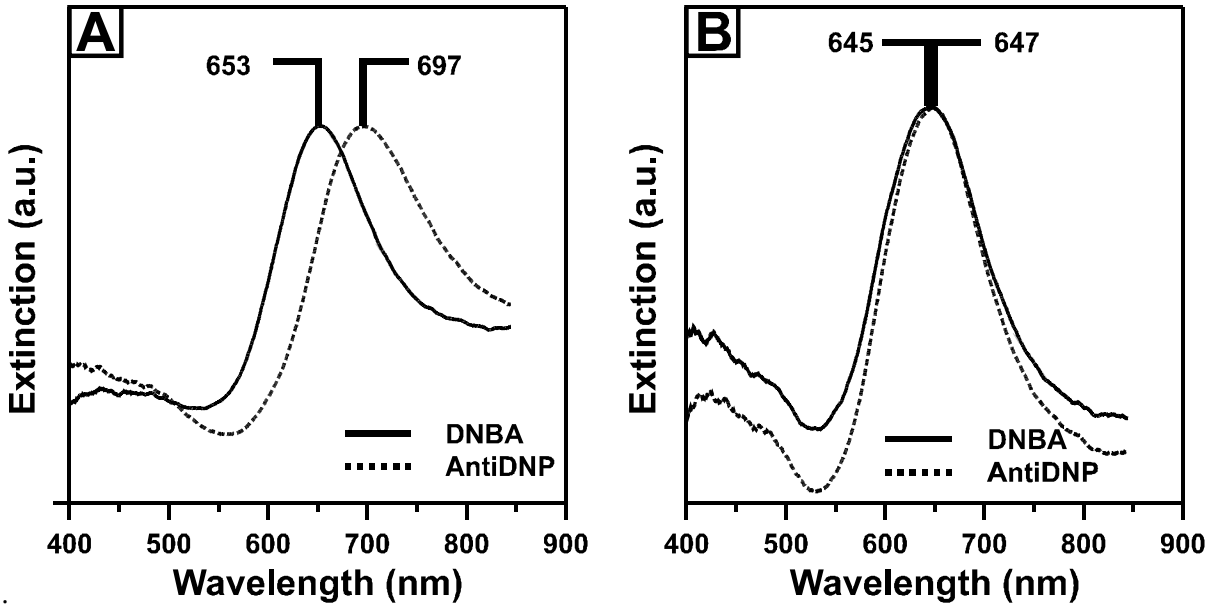

Figure 2: LSPR response of the Ag nanobiosensor to antiDNP concentration. All the measurements were taken in a nitrogen environment. (A) DNBA-functionalized nanoparticles (λ_{ex} = 653 nm) were exposed to 1.5 x 10^{-6} M antiDNP (λ_{ex} = 697 nm). (B) DNBA-functionalized nanoparticles (λ_{ex} = 645 nm) were exposed to 1.5 x 10^{-9} M antiDNP (λ_{ex} = 647 nm).

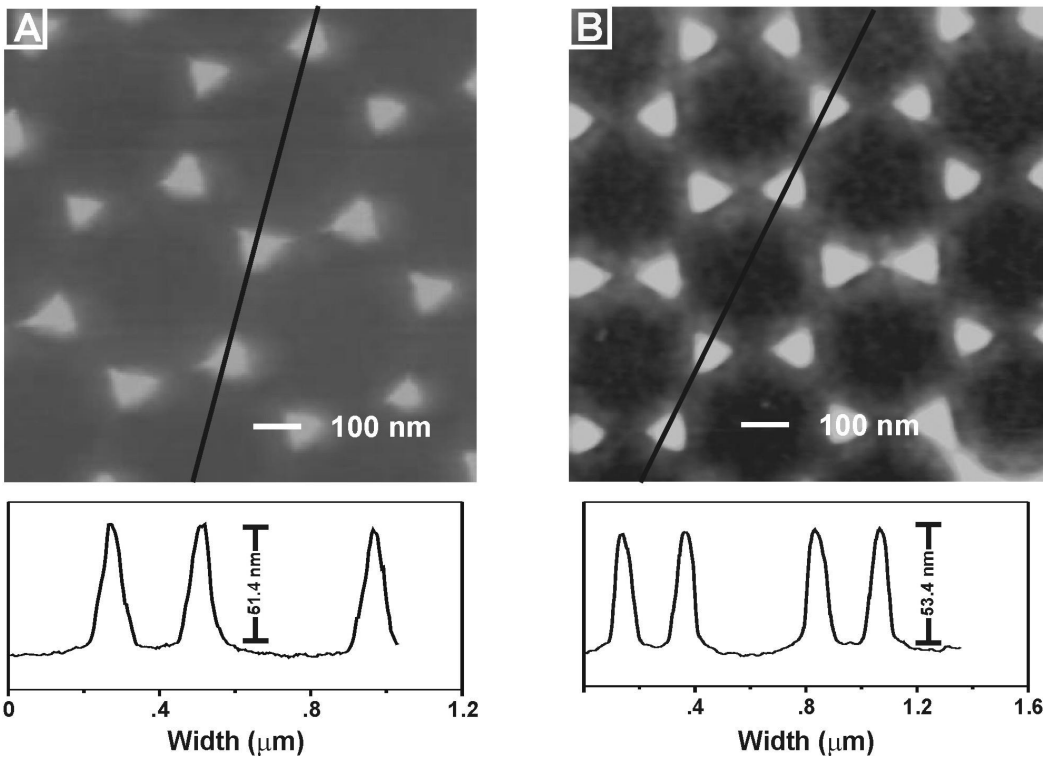

Figure 3. AFM tapping mode image and line scans of Ag nanosensors used to study the height increment after antiDNP binding. The Ag nanosensors were fabricated from hexagonal arrays of 390 nm diameter polystyrene spheres and 50 nm Ag deposition. (A) The Ag nanosensors were functionalized with SAM and DNBA (average height = 51.4 nm). (B) Ag nanosensors after exposure to 1.5 x 10^{-9} M antiDNP (average height = 53.4 nm).

represents the experimental data taken from a measurement on a different sample. The curve represents the calculated response given by Equation (2), [25]

$$\Delta R/\Delta R_{max} = K_{a,surf}[AD]/(1 + K_{a,surf}[AD]) \quad \textbf{(2)}$$

where ΔR is the LSPR response, ΔR_{max} is the maximum response, $K_{a,surf}$ is the surface binding constant, and [AD] is the antiDNP concentration. $K_{a,surf}$ was calculated to be 9.46 x 10^6 M^{-1} based on a best fit to the experimental data.

The binding curve provides three characteristics describing the binding of antiDNP to the DNBA-functionalized surface. First, the saturation point can be determined from the binding curve, which was estimated as 1.5 x 10^{-9} M. The commercial availability of antiDNP solutions dictated that 1.5 x 10^{-9} M was the highest antiDNP concentration that could be used in this study. Second, the detection is estimated to be less than 7.5 x 10^{-9} M. Finally, the response curve yields a surface binding constant of 9.46 x 10^6 M^{-1}, which is comparable to the literature value (4 x 10^6 M^{-1})[26] for antiDNP with spin labeled dinitrophenol.

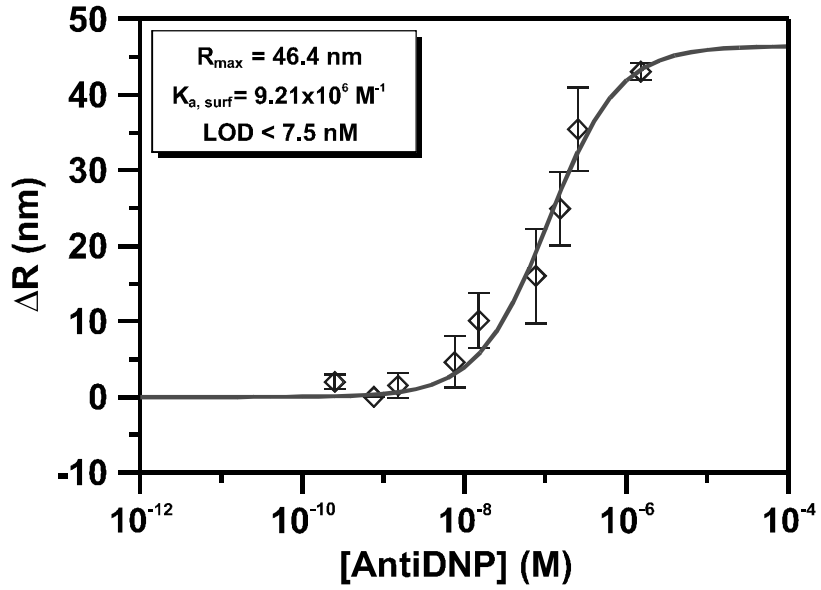

Figure 4. Maximum response (ΔR_{max}) vs. [antiDNP] curve when antiDNP binds to the DNBA-functionalized surface. The solid line is the calculated fit to the experimental data points. The calculated maximum response (R_{max}) is 46.4 nm, the binding constant at the nanoparticle surface ($K_{a,surf}$) is 9.21 x 10^6 M^{-1}, and the limit of detection (LOD) is less than 7.5 nM. Error bars display the total spread of the data.

3.3 SERS verification of the nanosensor fabrication. LSPR sensors detect surface binding or release of macromolecules; however, these sensors are unable to identify the chemical entity of the molecule that binds to the

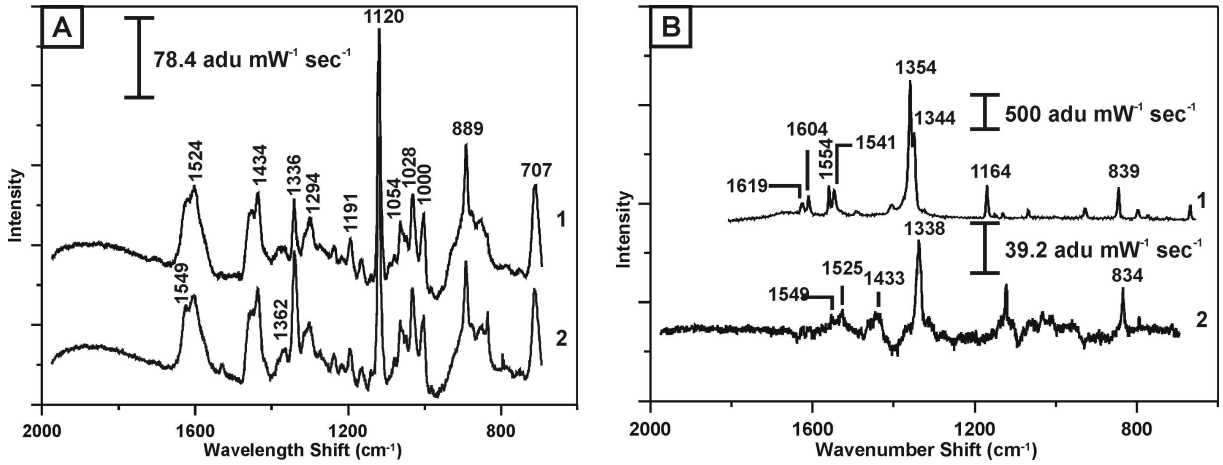

Figure 5: SERS spectra of the subsequent steps of the Ag nanotriangle surface during nanosensor fabrication. (A) SERS spectrum of SAM comprising of 1mM of 2:1 octanethiol : 11-aminoundecanol on AgFON (1) and SERS spectrum spectrum of 1 mM DNBA linked to the SAM (2). (B-2) Residual peaks representing amide bond formation obtained from subtracting (1) from (2), λ_{ex} = 632.8, P = 1.7 mW, acquisition time = 30 sec. (B-1) Raman spectrum of solid DNBA for comparison, λ_{ex} = 632.8, P = 1 mW, acquisition time = 10 sec.

surface. SERS on the other hand, is capable of revealing molecular characteristics of the analyte. SERS was used to verify each step of the nanosensor fabrication. In our preliminary studies, instead of using Ag nanoparticles as the substrate, AgFON was used because AgFON has a broad LSPR peak and a broad range of excitation wavelengths can be used for a SERS experiment. AgFON substrates were functionalized in the same manner as the Ag nanoparticles and all the SERS data were taken in ambient conditions after each step. Figure 5A.1 shows the SERS spectrum of the SAM-functionalized AgFON surface. The amine-terminated SAM was then linked with DNBA using an EDC linker. Figure 5A.2 shows the SERS spectrum of DNBA linked to SAM. Figure 5B.2 is the difference spectrum of the SAM spectrum from DNBA-linked surface (Figure 5A.1 – Figure 5A.2). Figure 5B.1 is the Raman spectrum of solid DNBA.

In Figure 5B.2, peaks at 1549 cm^{-1} and 1525 cm-1 are due to ring stretch from the benzene ring.[27] Peak at 1338 cm^{-1} represents the NO_2 stretch,[28] and 834 cm^{-1} characterizes C-N stretch of secondary nitro compounds.[29] Figure 5B.1 is the Raman spectrum of solid DNBA for comparision. Peaks seen at 5B.2, namely 1549 cm^{-1}, 1525 cm^{-1}, 1338 cm^{-1}, and 834 cm^{-1}, correlate with the peaks at 1554 cm^{-1}, 1541 cm^{-1}, 1354 cm^{-1}, and 839 cm^{-1} in the Raman spectrum. These preliminary SERS data reflects the presence of DNBA on the amine-terminated SAM. However, a series of experiment will be done to observe the intensity changes of the above-mentioned peaks by varying the concentration of the DNBA on amine-terminated SAM.

4. CONCLUSION

In this work, we have demonstrated that antiDNP can be detected quantitatively using Ag nanotriangles as LSPR nanosensors. The system used in this study is able to detect antiDNP from 1.5×10^{-6} M to 7.5×10^{-9} M. The surface-binding constant of antiDNP was calculated to be 9.46×10^{6} M^{-1}. Furthermore, each step of the fabrication of the LSPR sensor was confirmed using SERS. The vibrational band due to the benzene ring stretch, NO_2 stretch and C-N stretch also confirms the binding of 2-4 dinitrobenzoic acid with amine-terminated SAM.

5. ACKNOWLEDGEMENTS

The authors wish to acknowledge research collaboration with Adam D. McFarland. The authors also acknowledge the support of the nanoscale Science and Engineering Initiative of the National Science Foundation under NSF Award Number EEC-0118025.

6. REFERENCE:

(1) Van Der Merwe, P. A.; Barclay, A. N. "Analysis of cell-adhesion molecule interactions using surface plasmon resonance." *Curr. Opin. Immunol* **1996**, *8*, 257-261.

(2) Cunningham, B. C.; Wells, J. A. "Comparison of a Structural and a Functional Epitope." *J. Mol. Biol.* **1993**, *234*, 554-563.

(3) Johanson, K.; Appelbaum, E.; Doyle, M.; Hensley, P.; Zhao, B. "Binding Interactions of Human Interleukin 5 with its Receptor Subunit." *J. Biol. Chem.* **1995**, *268*, 20668-20675.

(4) Berger, C. E. H.; Beumer, T. A. M.; Kooyman, R. P. H.; Greve, "Surface Plasmon Resonance Multisensing." J. *Anal. Chem.* **1998**, *70*, 703-706.

(5) MacKenzie, C. R.; Hirama, T.; Deng, S. j.; Bundle, D. R.; Narang, S. R. "Analysis by Surface Plasmon Resonance of the Influence of Valence on the Ligand Binding Affinity and Kinetics of an Anti-carbohydrate Antibody."*J. Biol. Chem.* **1996**, *271*, 1527-1533.

(6) Brockman, J. M.; Frutos, A. G.; Corn, R. M. "A Multistep Chemical Modification Procedure To Create DNA Arrays on Gold Surfaces for the Study of Protein-DNA Interactions with Surface Plasmon Resonance Imaging." *J. Am. Chem. Soc*. **1999**, *121*, 8044-8051.

(7) Gotoh, M.; Hasegawa, Y.; Shinohara, Y.; Shimizu, M.; Tosu, M. "A New Approach to Determine the Effect of Mismatches on Kinetic Parameters in DNA Hybridization Using an Optical Biosensor." *DNA Res.* **1995**, *2*, 285-293.

(8) Malinsky, M. D.; Kelly, K. L.; Schatz, G. C.; Van Duyne, R. P. "Chain Length Dependence and Sensing Capabilities of the Localized Surface Plasmon Resonance of Silver Nanoparticles Chemically Modified with Alkanethiol Self-Assembled Monolayers." *J. Am. Chem. Soc.* **2001**, *123*, 1471-1482.
(9) Haes, A. J.; Van Duyne, R. P. "A Nanoscale Optical Biosensor: Sensitivity and selectivity of an Approach Based on the Localized Surface Plasmon Resonance Spectroscopy of Triangular Silver Nanoparticles." *J. Am. Chem. Soc.* **2002**, *124*, 10596-10604.
(10) Haynes, C. L.; Van Duyne, R. P. "Plasmon-Sampled Surface-Enhanced Raman Excitation Spectroscopy." *J. Phys. Chem. B* **2001**, *105*, 5599-5611.
(11) Kreibig, U.; Gartz, M.; Hilger, A. "Mie Resonances. Sensors for Physical and Chemical Cluster Interface Properties." *Ber. Bunsen-Ges.* **1997**, *101*, 1593-1604.
(12) Mulvaney, P. "Not all that's Gold does Glitter." *MRS Bulletin* **2001**, *26*, 1009-1014.
(13) El-Sayed, M. A. "Some Interesting Properties of Metals Confined in Time and Nanometer Space of Different Shapes." *Acc. Chem. Res.* **2001**, *34*, 257-264.
(14) Link, S.; El-Sayed, M. A. "Spectral Properties and Relaxation Dynamics of Surface Plasmon Electronic Oscillations in Gold and Silver Nano-dots and Nano-rods." *J. Phys. Chem. B* **1999**, *103*, 8410-8426.
(15) Kreibig, U.; Gartz, M.; Hilger, A.; Hovel, H. In *Adv. Met. Semicond. Clusters*; Duncan, M. A., Ed.; JAI Press Inc.: Stamford, 1998; Vol. 4, pp 345-393.
(16) Mulvaney, P. "Surface Plasmon Spectroscopy of Nanosized Metal Particles."*Langmuir* **1996**, *12*, 788-800.
(17) Jensen, T. R.; Kelly, K. L.; Lazarides, A.; Schatz, G. C. "Electrodynamics of Noble Metal Nanoparticles and Nanoparticle Clusters." *J. Cluster Sci.* **1999**, *10*, 295-317.
(18) Kreibig, U.; Vollmer, M. *Optical Properties of Metal Clusters*, 1995; Vol. 25.
(19) Jeanmaire, D. L.; Van Duyne, R. P. "Surface Raman Spectroelectrochemistry. Part I. Heterocyclic, Aromatic, and Aliphatic Amines Adsorbed on the Anodized Silver Electrode." *J. Electroanal. Chem.* **1977**, *84*, 1-20.
(20) Haynes, C. L.; Van Duyne, R. P. "Plasmon-Sampled Surface-Enhanced Raman Excitation Spectroscopy." *J. Phys. Chem. B* **2003**, *Web Release: 29 March 2003*.
(21) Kneipp, K.; Wang, Y.; Kneipp, H.; Perelman, L. T.; Itzkan, I.; Dasari, R. R.; Feld, M. S. "Single Molecule Detection Using Surface-Enhanced Raman Scattering (SERS)." *Phys. Rev. Lett.* **1997**, *78*, 1667-1670.
(22) Nie, S.; Emory, S. R. "Probing Single Molecules and Single Nanoparticles by Surface-Enhanced Raman Scattering." *Science* **1997**, *275*, 1102-1106.
(23) Schatz, G. C.; Van Duyne, R. P. *Electromagnetic Mechanism of Surface-Enhanced Spectroscopy*; Wiley: New York, 2002; Vol. 1.
(24) Shafer-Peltier, K. E.; Haynes, C. L.; Glucksberg, M. R.; Van Duyne, R. P. "Toward a Glucose Biosensor Based on Surface-Enhanced Raman Scattering." *J. Am. Chem. Soc.* **2003**, *125*, 588-593.
(25) Riboh, J. C.; Haes, A. J.; McFarland, A. D.; Yonzon, C. R.; Van Duyne, R. P. "A Nanoscale Optical Biosensor: Real-time Immunoassay in Physiological Buffer Enabled by Improved Nanoparticle Adhesion." *J. Phys. Chem. B* **2003**, *107*, 1772-1780.
(26) Anglister, J.; Frey, T.; McConnell, H. M. "Magnetic Resonance of a Monoclonal Anti-Spin-Label Antibody." *Biochem.* **1984**, *23*, 1138-1142.
(27) Sulk, R. A.; Corcoran, R. C.; Carron, K. T." Surface-Enhanced Raman Scattering Detection of Amphetamine and Methamphetamine by Modification with 2-Mercaptonicotinic Acid." *Appl. Spectrosc.* **1999**, *53*, 954-959.
(28) Han, H. S.; Han, S. W.; Kim, C. H.; Kim, K. "Adsorption and Reaction of 4-Nitrobenzoic Acid on -Functionalized Alkanethiol Monolayers on Powdered Silver: Infrared and Raman Spectroscopy Study." *Langmuir* **2000**, *16*, 1149-1157.
(29) Socrates, G. *Infrared and Raman Characteristic Group Frequnecies.*; John Wiley and Sons: Middlesex, UK, 2001.